NOVA SCHOOL OF
SCIENCE & TECHNOLOGY

DEPARTAMENT OF
MATERIALS SCIENCE

JOÃO AUGUSTO OLIVEIRA DE MARCO
BSc in Materials' Engineering

Additive manufacturing Of High Entropy Alloys

MASTER IN MATERIALS ENGINERRING
NOVA University Lisbon
September, 2023

DEPARTAMENT OF
MATERIALS SCIENCE

ADDITIVE MANUFACTURING OF HIGH ENTROPY ALLOYS

JOÃO AUGUSTO OLIVEIRA DE MARCO

BSc in Materials' Engineering

Adviser: João Pedro Oliveira
Assistant Professor, NOVA University Lisbon

Co-advisers: Isaque Moura
Doctoral Student, NOVA University Lisbon

Examination Committee:

Chair:

Rapporteurs:

Adviser:

Members:

MASTER IN MATERIALS' ENGINEERING

NOVA University Lisbon
September, 2023

ADDITIVE MANUFACTURING WITH HIGH ENTROPY ALLOYS

A chi c'è sempre stato
A chi se né andato.
A chi ha creduto in me fin dall'inizio.
E fino alla fine.
A te che più chiunque altro avresti voluto esserci.

Ai miei genitori e alla mia famiglia.

Acknowledgments

First of all, I would like to start thanking my supervisors and co-advisors, Professor João Pedro Oliveira, Doctoral Students Isaque Moura and Jiajia Shen, for their help and support during these last months. Thank you for always give me the best guidance, for presenting me with valuable information and challenges and calming me down when necessary. I would like to say thank you to all people in CENIMAT and DEMI for the hours made available to teach me how to use all the machinery as well as to improve my laboratory skills.

I would like to say thank you to all my family for always believing in me and encouraging me to never stop dreaming and never give up. A special thank you to my father for all the work he put on for making all this 5 years journey possible and for always support me in everything.

A big thank you to my friends for being there for 5 years and help me and put up with my stuff and never run away.

Could not finish without give a big thank you to my girlfriend for being my biggest supporter and believer and to her family for all the support given to me, and for making me feel like family.

I wish to convey to everyone I've mentioned that these words come sincerely from the depths of my heart, and I truly appreciate each and every one of you

"It is hard to fail, but it is worse never to have tried to succeed." (Theodore Roosevelt).

ABSTRACT

High-entropy alloys (HEAs) have garnered recent attention as a novel class of advanced engineering alloys due to their capacity for compositional control, microstructure manipulation, and tailoring of mechanical properties. Similarly, additive manufacturing (AM) has also witnessed a surge in interest. AM is a process for fabricating physical objects by layer-by-layer assembly from digital designs. This innovative technology has the potential to revolutionize the paradigm of product design, fabrication, and distribution by enabling complex geometries, on-demand production, and just-in-time manufacturing.

This study presents an analysis of a new alloy (Fe40Mn20Co20Cr15Si5) fabricated using the Laser Powder Bed Fusion (LPBF) method. The primary objective was to investigate the effects that printing parameters may exert on the resulting samples. To achieve this, a comparative study was conducted involving two samples with varying parameters (power and scanning speed). Two distinct types of analyses were employed for this comparison: microstructural analysis and mechanical property assessment.

Microstructural analysis of the samples was carried out using optical microscopy, involving various magnifications and pre- and post-treatment processes (etching). However, it was determined that this method was insufficient to fully elucidate the microstructure.

Furthermore, mechanical property analysis consisted of two distinct studies involving hardness tests and compression tests on the samples. These tests revealed notable differences in material behaviour with respect to the employed printing parameters.

Keywords: High Entropy Alloys, Additive Manufacturing; Printing Parameters; laser Powder Bed Fusion; Mechanical Properties; Microstructure.

Resumo

Ligas de alta entropia (HEAs) têm recebido atenção recente como um novo tipo de ligas de engenharia avançadas devido à capacidade de controlar sua composição, microestrutura e propriedades mecânicas. O mesmo aconteceu com a manufatura aditiva. MA é um processo de criação de objetos físicos montando-os camada por camada a partir de um projeto digital. Essa tecnologia inovadora pode potencialmente alterar a metodologia de como produtos são projetados, fabricados e distribuídos, permitindo geometrias complexas, produção sob demanda e fabricação "just-in-time". Neste trabalho foi feito uma análise sobre uma nova liga (Fe40Mn20Co20Cr15Si5) impressa pelo método de LPBF (Laser Powder Bed Fusion). Teve como principal objetivo, observar os efeitos que os parâmetros de impressão podem ter nas amostras. Para tal foi feita uma comparação entre 2 amostras com parâmetros diferentes (Potencia e velocidade de impressão). De forma a comparar estas duas amostras foram feitos dois tipos de análises, análise da microestrutura e das propriedades mecânicas das amostras.

A análise da microestrutura das amostras foi feita utilizando o método de Microscopia Ótica, com diversas ampliações e pré e pós tratamento (Etching), no qual foi possível concluir que era uma análise insuficiente para poder observar microestrutura.
Para a análise das propriedades mecânicas, dois estudos foram realizados. Foram feitos testes de dureza e ensaios de compressão as amostras. Foi possível observar as diferenças do comportamento do material consoante os seus parâmetros de impressão.

Palavas chave: Ligas de alta entropia; manufatura Aditiva; Parâmetros; *Laser Powder Bed Fusion*; Propriedades mecânicas; Microestrutura;

CONTENTS

LIST OF FIGURES

LIST OF TABLES

ACRONYMS

HEA	High Entropy Alloy
AM	Additive Manufacturing
CS-HEA	Complex Structured High Entropy Alloy
HCP	Hexagonal Close-packed
FCC	Face Centered Cubic
LPBF	Laser Powder Bed Fusion
SLM	Selective Laser Melting
SLS	Selective Laser Sintering
WAAM	Wire and Arc Additive Manufacturing
LAM	Laser additive manufacturing
VED	Volumetric Energy Density

SYMBOLS

γ	Called gamma, it refers to austenite phase.
$\boldsymbol{\varepsilon}$	Called epsilon, it refers to martensite phase.
P	Power (normally in watts)
v	Speed (normally in m/s, in this case mm/s)
h	Distance between layers (mm)
d	layer thickness (mm)

1

INTRODUCTION

1.1 High Entropy Alloys

High entropy alloys (HEAs) have recently been gaining attention as a new type of advanced engineering alloys because of the ability to control their composition, microstructure, and mechanical properties[1]. HEAs are a type of metallic material that is characterized by its high degree of chemical disorder or randomness. This is achieved by combining at least five main elements, resulting in an alloy with a high degree of chemical complexity. [2]

The origins of this concept can be traced back to 2004 [3], [4], when the first research on the subject was published. B. Cantor et al [3] were the firsts to try an initial attempt to investigate the multicomponent alloy area. The first alloy investigated contained 20 elements (Mn, Cr, Fe, Co, Ni, Cu, Ag, W, Mo, Nb, Al, Cd, Sn, Pb, Bi, Zn, Ge, Si, Sb, Mg) in equal atomic proportions of 5 at. % each. The second alloy contained all the elements above excluding Bi, Ge, Si and Sb. Each 16 with equal atomics composition of 6.25 at.%. Further investigation focused on studying the single-phase field of a multicomponent fcc structure. This involved creating a five-component alloy with 20 at. % of Cr, Mn, Fe, Co, and Ni each.[3]

After these first alloys investigated, they focused on a 5 elements alloy (Fe, Cr, Mn, Ni, Co) with additions of Nb, Ge, Cu, Ti and V. Since this first investigation, many other studies have been conducted to add to existing knowledge of HEAs. [5], [6]

High entropy alloys (HEAs) have several unique characteristics that sets them apart from other materials. These include:

- (i)The high-entropy effect, which is related to the entropy of the material's atomic configuration.
- (ii) Slow diffusion, which results in better high-temperature properties compared to conventional alloys.
- (iii) Significant lattice distortion, caused by the presence of at least five atoms with different sizes.
- (iv) The cocktail effect, where the addition of certain elements can greatly enhance specific properties of the alloy.[7]

Welding of materials related to High Entropy Alloys (HEAs) is a relatively unexplored field, currently in the experimental phase within laboratory settings. To enable the practical use of materials related to High Entropy Alloys (HEAs), it is essential to investigate various welding techniques. To date, researchers have explored and studied several welding methods, which can be categorized into three primary groups: [8]

- Fusion-based weld techniques;
- Solid-state welding techniques;
- Diffusion reacted -based weld techniques.

The weldability of HEAs can also be influenced by factors such as the specific alloy composition, the welding procedure being used, and the material's microstructural properties. Some HEAs may be more difficult to work with than others and some have been found to be unsuitable for welding, such as those with low melting point components like aluminium or magnesium that may melt during the welding process, leading to flaws in the weld.[8]

One of the key benefits of HEAs is their ability to exhibit a wide range of desirable mechanical and physical properties. For example, many HEAs have a high strength-to-weight ratio, making them ideal for use in structural applications where weight is a concern. Aluminium-based HEAs, have the main element aluminium combined with lightweight elements like magnesium and lithium, these alloys are known for their low density and high strength. They also have a high melting point and good corrosion resistance, making them suitable for high temperature and harsh environments. [9], [10]

In addition to their practical applications, high entropy alloys are also of interest to researchers due to their unique microstructural and physical properties. These properties are a result of the high degree of chemical disorder in the alloy, which leads to a wide range of possible configurations of atoms at the microscopic level. This makes HEAs a promising material for a variety of advanced applications, such as in energy storage and conversion, catalysis, and electronics.[10]

There are a few different examples of high entropy alloys in use today. One example is the aluminide-based high entropy alloy (Al-HEA), which is used in the aerospace industry for its high strength and corrosion resistance at elevated temperatures. Another example is the cobalt based high entropy alloy (Co-HEA), which is used in biomedical applications due to its biocompatibility and ability to resist corrosion in the body. [11]–[13]

As research into these materials continues, it is likely that they will find even more practical uses in the future.

1.2 Additive Manufacturing

Additive manufacturing is a process of creating physical objects by assembling them layer by layer from a digital design. This innovative technology can potentially change the methodology of how products are designed, fabricated, and distributed, by allowing for complex geometries, on-demand production, and just-in-time manufacturing. [14]

The common format for this type of file is a computer-aided design (CAD) file. This file is then transformed into a stereolithography (STL) file, which has data on every layer that needs to be printed and approximates the drawing made in the CAD software using triangles. This data is then used to guide the additive manufacturing process, building up the object layer by layer until it is complete. [14]

The ability of additive manufacturing technology to create complex structures has had a big impact on the manufacturing industry. There are several different methods for additive manufacturing of metals, such as selective laser melting (SLM) and selective laser sintering (SLS) that use powdered materials and use a high-power laser to selectively melt and fuse metal powder particles layer by layer. Among these methods there is wire and arc additive manufacturing (WAAM) which uses wire materials and an electric arc as a heat source to melt a continuous wire feedstock.

SLM and SLS can produce parts with smooth finishes but have a slow production rate. WAAM has a faster production rate, but the parts it creates have rough surfaces. The implementation of non-destructive testing is critical for industrial use of additive manufacturing, but it is challenging due to the complex shapes and rough surfaces of parts made with additive manufacturing. [15]

There are several additive manufacturing methods that are commonly used as illustrated in Figure 1: [14], [16]

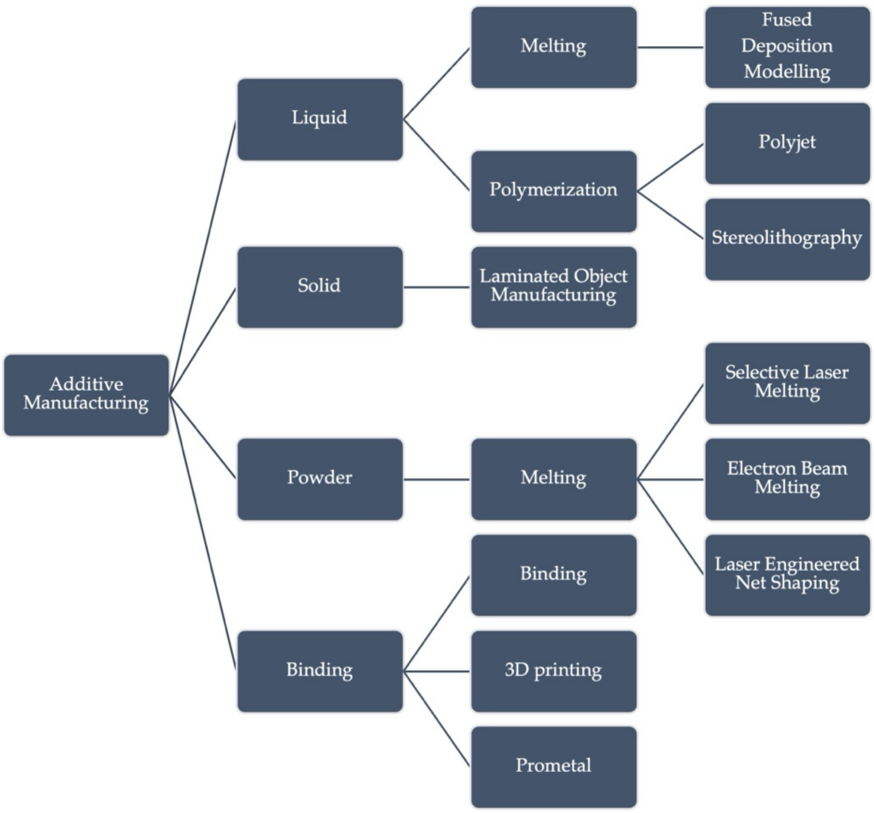

Figure 1 - Addittive Manufacturing Methods

Additive manufacturing has a significant advantage over traditional methods in that it allows for the rapid and cost-effective creation of intricate and specialized products. Whereas traditional techniques often need the manufacture of moulds or dies, which can be costly and take a long time, additive manufacturing can directly produce the final product, eliminating the need for these intermediary steps. [17]

Another benefit of additive manufacturing is its sustainability emphasis, it has the potential to reduce waste and reduce the energy consumption. In traditional manufacturing, a large amount of material is often discarded as scraps or offcuts. With additive manufacturing, the amount of material used can be precisely controlled, reducing waste, and lowering the overall cost of production. [17]

The use of additive manufacturing is not limited to the production of physical objects. It is also being used to create structures and systems that are not possible with traditional manufacturing methods. Researchers are using additive manufacturing to create customized prosthetics and implants for medical applications, the titanium alloy Ti_6Al_4V is one of the many examples. This alloy, processed by LAM (Laser additive manufacturing) is mostly used for joint replacement due to its good mechanical properties (good biocompatibility, high fatigue resistance and good osseoconductivity). [18][19]

As well as to build structures for use in space exploration. Structural parts in spacecrafts have the necessity to stand up to difficult conditions and due to that good mechanical properties are needed. This is when metal 3D printing comes, the possibility to build a structure lightweight with the shape wanted and with the mechanical properties required. [12]Orme et al, used selective laser melting to produce AlSi10Mg components for a satellite. [12], [20]

Additionally, additive manufacturing offers environmental advantages. Enabling the production of items in closer proximity to their point of use can diminish the necessity for transportation, thereby decreasing the carbon emissions linked to the transportation of goods. [14], [17]Additive manufacturing is inherently more efficient in terms of material usage compared to traditional manufacturing methods. It adds material layer by layer, resulting in less waste compared to subtractive methods that remove material to shape a product.

Additive Manufacturing, while offering numerous benefits, presents several challenges. A primary limitation resides in the material selection for the process. Although AM accommodates a broad material range, not all materials possess suitable properties for every application. Additionally, high equipment costs and industry standardization gaps act as barriers to broader adoption. [21]

The lack of technical standards stands out as a significant impediment to AM adoption. These challenges, including material constraints, cost considerations, and the absence of industry-wide standards, partly result from the technology's early developmental stage. It is imperative for managers and product engineers to recognize these challenges and the developmental context when assessing AM's potential integration into conventional design methodologies. [22]

Overall, additive manufacturing is a cutting-edge technology with the potential to revolutionize the process of designing, producing, and delivering products. As the technology continues to evolve and gain more widespread usage, it is likely to have a considerable effect across many different industries and fields.

1.3 State of the art

Alloys renowned for their exceptional strength have long grappled with a common challenge – the lack of ductility, often stemming from inadequate work hardening and premature initiation of damage. In response to this persistent issue, a remarkable new material has emerged: the metastable $Fe_{40}Mn_{20}Co_{20}Cr_{15}Si_5$ CS-HEA (Complex Structured High Entropy Alloy), crafted using the laser powder bed fusion additive manufacturing technique. [23]

This pioneering material boasts a unique microstructure that sets it apart. Within its composition, one can observe ultrafine f.c.c. (face-centered cubic) γ grains intricately embedded within a refined hexagonal closed packed (h.c.p) ε matrix. What distinguishes this material is the transformative behavior of the γ phase and the presence of twinning in the ε phase. These phenomena, rather than compromising the material's ductility, contribute to an equitable distribution of strain between the phases. The outcome is remarkable: sustained strengthening without any sacrifice in ductility.[9], [23]

Further exploration conducted by Agrawal and their team [23] has unveiled a new iteration of this material, its composition is shown in Table 1. In this version, the ε-h.c.p. phase predominantly governs the microstructure. This material was manufactured using the LBPF system Aconity MIDI. To produce this CS-HEA, the following parameters were employed: a laser power of 140 W, a hatch spacing of 0.1 mm, a layer thickness of 0.04 mm, a scanning speed of 800 mm/sec, and a rotation angle of 67 degrees between adjacent layers. [23] The printing process was conducted in an argon protective atmosphere with oxygen content maintained below 0.01% throughout the entirety of the laser powder bed fusion (LPBF) process. This discovery underscores the adaptability and versatility of CS-HEAs in fine-tuning their microstructural characteristics to achieve specific mechanical properties. It is a testament to the vast potential these materials hold across a spectrum of applications. [6], [23]

Table 1 - Chemical composition of the pre-alloyed powder.

Elements	Cr	Co	Si	Mn	Fe
at. % (Nominal)	15	20	5	20	40
at. % (Actual)	14.8 ± 1	19.1 ± 1.16	5.5 ± 0.4	18.8 ± 1.08	41.8 ± 1.10

In summary, the metastable $Fe_{40}Mn_{20}Co_{20}Cr_{15}Si_5$ CS-HEA represents a significant breakthrough in materials science, addressing a long-standing challenge in alloys with high strength. Its unique microstructural features, combined with the transformative behavior of its constituent phases, promise to revolutionize the landscape of high-strength, high-ductility materials for diverse industrial applications. This innovative alloy stands as a testament to the progress and ingenuity in materials engineering. [24]

2

MATERIALS AND METHODS

2.1 Printing

Pre-alloyed CS-HEA ($Fe_{40}Mn_{20}Co_{20}Cr_{15}Si_5$ (at. %)) was gas atomized at Oerlikon Metco with powder particle size in the range of 15–50 μm. The chemical composition of powders is shown in Table 1.

Table 1 - Chemical composition of gas atomized CS-HEA powder.

Elements	Fe	Mn	Co	Cr	Si
at. % (Nominal)	40	20	20	15	5
at. % (Actual)	41.8	18.8	19.1	14.8	5.5

The LPBF process was conducted using TRUMPF (Truprint 1000) with a maximum 200 W laser with spot size 55 μm. An inert argon atmosphere with oxygen content below 100ppm (0.01%) was used. The printed parameters used as well as sample nomenclature are shown in Table 2; scan rotation of 67° was used between alternating layers. The printed rectangular blocks were built with dimensions of 10mm long, 22 mm wide, and 22 mm thick. To calculate the volumetric energy density, the follow formula was used:

Equation 1 - Volumetric energy density equation

$$VED = \frac{P}{\text{vhd}} \left(\frac{J}{mm^3}\right)$$

P – Power (W)
v – speed (mm/s)
h -Distance between layers (mm)
d – layer thickness (mm)

Table 2 - LPBF process parameters used for the present work.

Sample Nº	Power (P, W)	Scanning speed (V, mm/s)	Hatching space (H, mm)	Layer thickness (L, mm)	Volumetric energy density (VED, J/mm^3)
1	180	1000	0.1	0.04	45
2	170	800	0.1	0.04	53.125

2.2 Analyse Preparation

2.2.1 Cutting

Samples from both build and transverse directions were obtained by cutting with linear precision saw IsoMet 4000 Linear Precision Saw from Buehler (Blade speed of 1500 rpm and a feed rate ranging from 4.5 mm/min to 5.5 mm/min) with a diamond cutting disc, resulting in 4 samples to analyse.

2.2.2 Etching

Etching is a chemical process that acts in a sense of corrode the places with higher energy and deformation. In this case the grain boundary, which is why it is possible to visualize the microstructure. In this case the etching was done with two solutions. The first solution was a 3:1 HCl/HNO3 with 15mL to 5 mL. The second one was Keller's solution but was only done in the sample 1 transversal direction.

2.3 Material characterization

2.3.1 Optical Microscopy

To obtain the smooth surface to analyse via optical microscopy the samples were polished with paper sand (400 to 4000), and finished with diamond paste (3 □m)

This was the first process to analyse the samples. It was used an inverted reflected light microscope, Leica DMI5000 M. The process was done by beholding the sample in the screen to observe some trace elements of different microstructure.

2.3.2 Hardness Testing

This method involves a non-destructive procedure wherein a load is exerted using a pointed tip to create an indentation on the sample in a desired distance range. This test was done by Vickers microhardness method where it involves pressing a precisely shaped diamond indenter into the sample. In this case the load used was 500g and the distance between each indentation was every 20 μm until getting a decent number of values to analyse. The distance between each indentation must follow a technical standard (ISO 6507-1, 2018). This process was done in by a Mitutoyo Micro Hardness Testing Machine HM-112.

2.3.3 Compression Testing

Compression testing consists in a mechanical testing made for mostly brittle materials. Is usually done to assess how a material responds when subjected to compressive loads. Throughout the testing process, different characteristics of the material are computed and represented graphically in a stress-strain chart. This chart is then utilized to ascertain attributes like elastic threshold, proportional threshold, yield point, yield strength, and, in certain cases, compressive strength.

In this work a Universal Mechanical testing Machine was used: Shimadzu AG-50kNG. The samples were cut in the following dimensions:

Sample 1: 3x3x4.2 (mm) BD
3x3x5.4 (mm) TD
Sample 2: 4x4x6 (mm) BD and TD

The parameters used for this test were a maximum load of 50kN an d a loading speed of 1mm/s.

3

RESULTS AND DISCUSSION

3.1 Optical Microscopy

3.1.1 Before Etching

The specimens underwent initial assessment using optical microscopy, as depicted in Figure 2. This preliminary examination allowed for an evaluation of the print quality prior to etching. Each sample exhibited distinct degrees of densification,Table 2, thereby resulting in variations among them in terms of structural defects. The samples densification was measured using the Archimedes' Principle. Generally observed across the samples were the presence of pores and instances of lack of fusion at specific points.

Table 2 - Sample Densification

Sample	ρ (%)
1	96,99
2	98,85

Figure 2 (a) it is possible to see some little points here there was some lack of fusion but mainly what it is possible to see is some scratches from the grinding and bad polishing whereas Figure 2 (b) shows a smoother surface. Figure 2 (b) shows a lot of pores and few points where there was lack of fusion.

In Figure 2 (c) and Figure 2 (d) show a similar aspect. It can be seen some points where there was lack of fusion and some pores as well.

These irregularities could be avoided by changing the printing parameters. Changes that could be more power used or less speed in the printing or even less hatch spacing.

(a) Sample 1 Building Direction (b) Sample 1 Transversal Direction

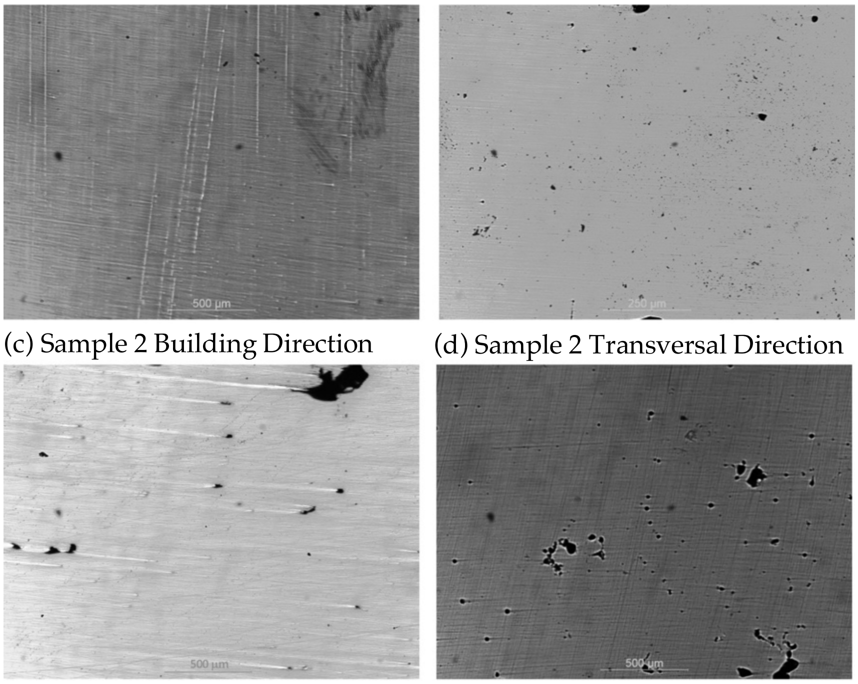

(c) Sample 2 Building Direction (d) Sample 2 Transversal Direction

Figure 2 - OM images of the samples before etching

3.1.2 After Etching

Analysing the sample microstructure with only Optical Microscopy is hard due to the grain being very refined owing to the extremely cooling rates of LPBF. However, it is possible to observe some characteristic of the material and some phenomena. All images from **Erro! A origem da referência não foi encontrada.** had a similar behaviour, in all of them it is possible to see melt pools and the boundaries. This is the primary effect of the interaction between a laser and a material, and its characteristics significantly influence heat transfer, solidification patterns, and the creation of defects. The intense heat causes the material to rapidly melt and fuse together, creating a small, controlled pool of molten material.[25], [26]

In all of images below, the mainly phenomena being shown is the melt pools, indicated in orange in Figure 3. Most of the images is the only data we can see. There´s also some trace elements that could mean some microstructure but as it was said before, it is difficult to observe is the rain size and this magnification.

Though most images show the same behaviour, in Figure 4 (d) there is a different phenomenon happening, it is what is called the Marangoni effects. This effect often occurs within melt pools. It is related to surface tension variations in a liquid.

Marangoni effects within melt pools result from surface tension fluctuations due to temperature differences. These effects induce the movement of molten material from warmer to cooler areas within the pool, thereby affecting the mixing and distribution of the material. In the realm of 3D printing, Marangoni effects play a role in shaping the melt pool, regulating temperature uniformity, and influencing solidification patterns. They may also play a part in the formation of imperfections like uneven surfaces and porous regions in the final printed objects. Managing Marangoni effects through process parameters is essential for enhancing the quality of printed outputs.[27] Figure 3 (d) is the only image where it is seen this behaviour, where the different colours in the image show different compositions in the material.

It was observed the presence of twins within the material. The appearance of twins is indicative of a TWIP-related transformation, where localized deformation and strain result in the formation of twin boundaries. These twins enable the material to undergo significant plastic deformation before eventual fracture, making TWIP alloys highly desirable for applications requiring high strength and impact resistance. [28]

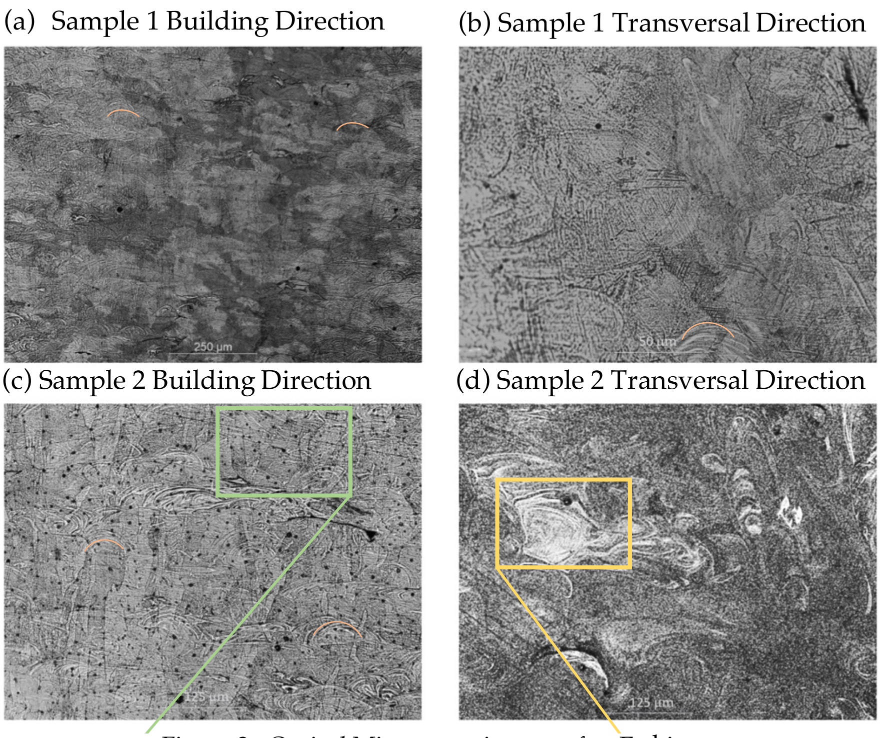

Figure 3 - Optical Microscopy images after Etching

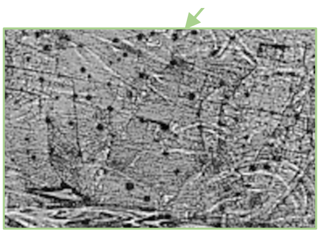

Figure 5 - Twins happening in the sample.

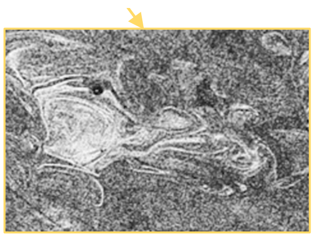

Figure 4 - Marangoni Effect.

3.2 Hardness Test

The Vickers microhardness test was done in the pursuit of a better comprehensive understanding of the material behaviour and properties. This test is important as it provides with value information of the material such as its mechanical strength, wear resistance and overall durability. For calculating the Vickers hardness number (HV) the following formula is used:

Equation 2 - Vickers Microhardness Number equation

$$HV = 1{,}854 \times \frac{F}{d^2}$$

HV-Vickers Hardness number
F – Applied Force
D - diagonal length of the indentation

Using this method of hardness testing provides some advantages such as, the load applied in the sample is a uniform load, making it less sensitive to surface irregularities and can be used in a wider range of materials.

The results obtained were the follow, Figure 6, Figure 7. For the first sample Figure 6 (1 Building Direction), the test started from the first layer, which is why the highest value of HV was in the beginning of test. This phenomenon happens due to the higher temperature gradient in the very beginning of the printing. The temperatures difference between the first layer deposited and the printing platform creates a harder phase, in this case Martensite. HCP is created to these higher heat extraction phenomena. This phenomenon gradually stops happening because this difference between the temperatures start to decrease and the HV. Despite not having a trend line, in Figure 6, it is possible to observe throughout the length of chart a decrease in HV values. However, there are some points that oscillate. These oscillating points can show areas of the sample where martensite is not present but γ-phase instead.

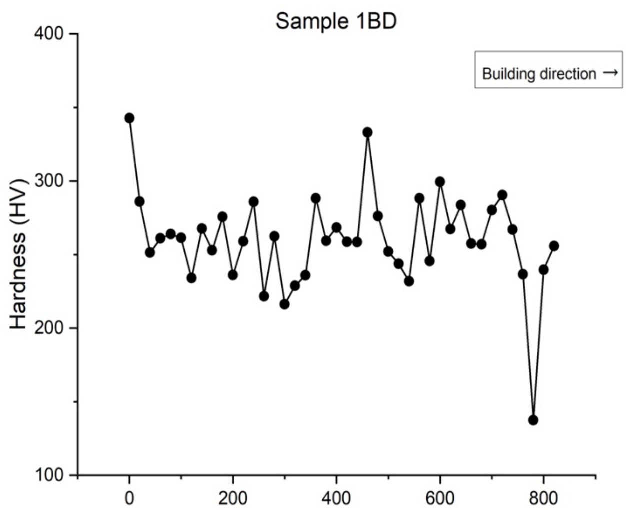

Figure 6 - Hardness Test - Sample 1 Building direction

Figure 7 shows the results from the second sample (2 Building direction). Opposite to the first sample, this test was started from the top layer of the sample, thence the HV values start at a lower value. Comparing with the test in Figure 6, it is possible to see a similar behaviour despite both tests been started from opposite areas. The HV values increase, showing points where HV is higher, corresponding to martensite phase, whereas lower values of HV, correspond to γ-phase.

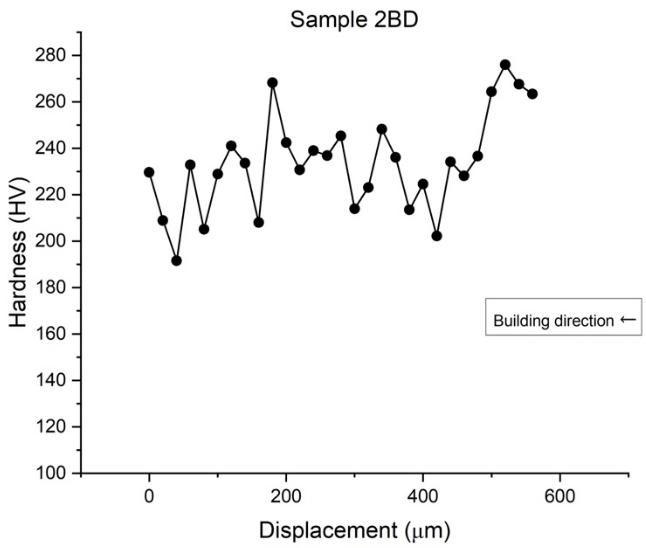

Figure 7 - Hardness Test - Sample 2 Building direction

Observing the results, it shows that the sample 1, printed with a higher power (180W) and higher speed (1000mm/s) had a higher HV value compared to sample 2, printed with power of 170 W and a speed of 800 mm/s.

3.3 Compression Test

Compression tests are fundamental experiments in materials science and engineering used to characterize a material's response to axial compressive forces. These tests provide crucial insights into a material's mechanical behavior, including its compressive strength, elastic modulus, and ductility. By subjecting specimens to controlled loading conditions, compression tests reveal how materials deform under compressive forces and offer valuable data for design and structural analysis.

In order to secure a better analyse of each sample, several values were obtained and calculated. The ultimate compressive strength was obtained using Equation 3; and the young's' Modulus and the yield strength using the 0,2% offset method.

Equation 3 - Compressive Strength equation

$$\sigma_c = \frac{P}{A}$$

σ_c-Ultimate compressive strength (MPa)
P-Maximum load (kN)
A- Cross-Sectional Area (mm^2)

Analysing the outcomes derived from each sample in each orientation, a congruent behaviour was discernible in both specimens, notwithstanding the dissimilarity in their numerical values. Each region exhibits pronounced delineation, facilitating their unequivocal identification: The elastic region, the plastic region, and the region culminating in structural failure, even though the sample remained intact.

This chart illustrates the mechanical response of Sample 1, as shown in Figure 8, when subjected to increasing loads. The curve on the chart displays clear regions, including an initial linear elastic phase, a yielding phase marked by plastic deformation, and a point at which ultimate failure occurred. Sample 1 successfully withstood the applied load without experiencing structural failure. The yield strengths were determined to be 767 MPa and 623 MPa for Sample 1BD and 1TD, respectively. Additionally, the ultimate stresses reached 1479 MPa and 2435 MPa for the same respective samples. The chart follows the expected stress-strain behaviour characteristic of this material.

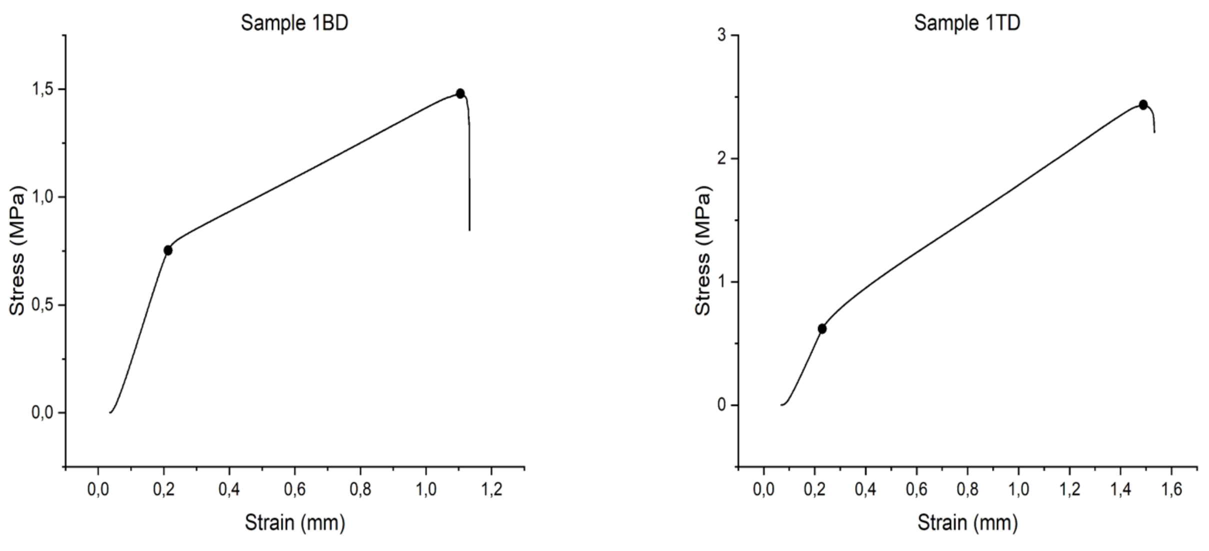

Figure 8 - Sample 1 Compressive Test

This compression test chart presents the mechanical behaviour of Sample 2, **Erro! A origem da referência não foi encontrada.**, under increasing load. The curve exhibits distinct zones: an initial linear elastic region, a yielding region characterized by plastic deformation, and an ultimate failure point. Sample 2 withstood the applied load without breaking. The yield strength was determined to be 334 MPa and 590 MPa, to sample 2BD and 2TD respectively. The ultimate stress reached 1159 MPa and 1686 MPa. The curve follows a typical stress-strain behaviour for this material.

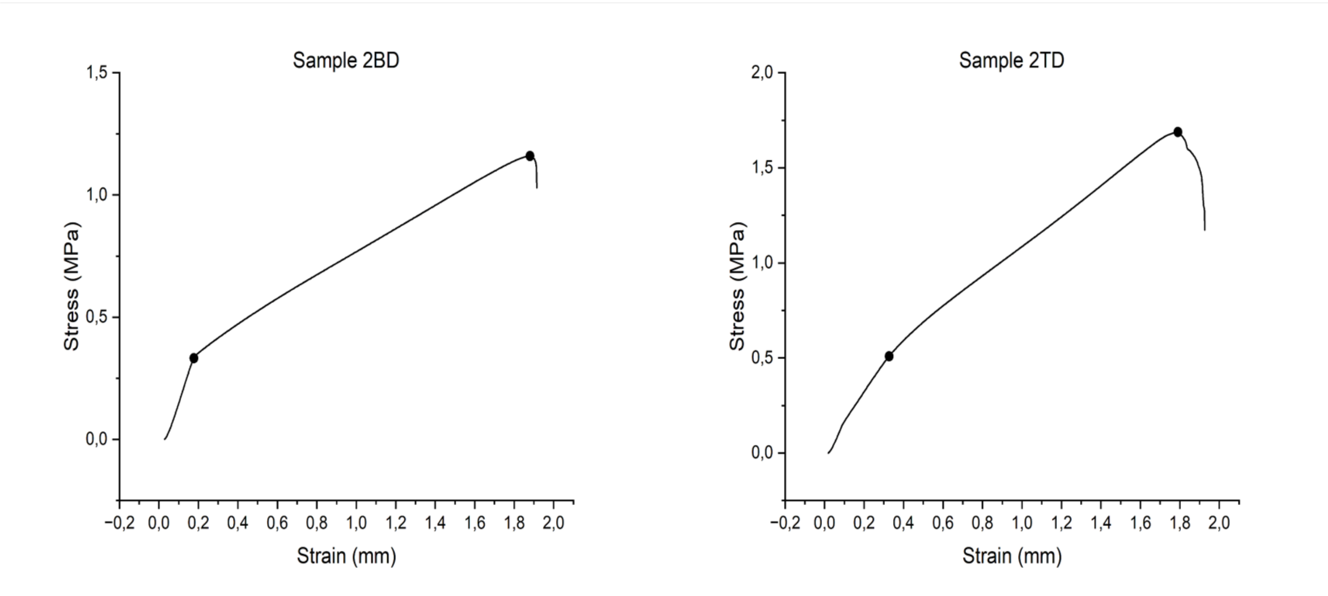

Figure 9 - Sample 2 Compression Test

In comparing the compressive strength of the samples, Table 3 it is discernible that the sample with lower porosity exhibits a superior compressive strength. This observation implies that an increased level of porosity can compromise the material's structural integrity, resulting in a diminished load-bearing capacity.[29], [30]

Table 3 - Ultimate compressive Strength of each sample

Sample	σ_c (MPa)
1BD	1,479
1TD	2,435
2BD	1,159
2TD	1,686

Upon analysing the deformation characteristics of the samples, it becomes evident that a sample with lower porosity is likely to demonstrate a more ductile behaviour, featuring greater plastic deformation before reaching the point of failure. Conversely, higher porosity tends to induce a more brittle fracture behaviour. [30]

The distinct porosities exhibited by two samples have yielded crucial insights into the material's mechanical behaviour. This indicates a clear inverse relationship between porosity and yield strength. The sample with higher porosity exhibited a reduction in yield strength, emphasizing the detrimental effect of increased voids on load-bearing capacity.

Table 4 - Yield Strength of each sample

Sample	**σ_y (MPa)**
1BD	0,767
1TD	0,623
2BD	0,334
2TD	0,509

In our compression test scenario, the differences in porosity between the two samples are associated with differences in Young's Modulus as well. Young's Modulus, representing material rigidity, displays an inverse relationship with porosity. Specifically, the sample featuring lower porosity showcases a higher Young's Modulus, indicating its superior capacity to resist deformation under applied stress and promptly revert to its initial configuration upon load removal. [31] Despite having some results of Young’s Modulus, these values were not the most accurate due to the accuracy of the compression test machina.

It is worth noting that the samples, owing to their high hardness, did not undergo fracture.

When assessing the energy absorption capacity of each sample, it is probable that samples with lower porosity will exhibit a higher capacity to absorb energy during deformation. Consequently, they are better suited for applications involving impact or the dissipation of energy.

Consideration of the intended application of the high entropy alloy is imperative. Depending on the specific requirements of the application, one sample may be more suitable than the other. Lower-porosity alloys are likely to be preferred for load-bearing or structural applications, while higher-porosity alloys may offer advantages in certain lightweight or energy-absorbing applications. [29]

These conclusions hold the potential to inform material selection and processing decisions tailored to distinct applications and can provide valuable insights for future research endeavours aimed at enhancing the properties of these alloys.

4

CONCLUSIONS

In this study, we explored the realm of additive manufacturing of high entropy alloys. The investigation aimed to shed light on the relationship between the densification of printed samples and their resulting mechanical and microstructural properties. Through a comprehensive series of experiments, we have gained valuable insights into the capabilities and limitations of this cutting-edge technology.

Our optical microscopy analysis provided a better understanding of the microstructure of the printed samples. However, it was not possible to analyse the microstructure in full detail. It was observed some phenomena happening in the samples but not the microstructure itself. This information is crucial for tailoring the properties of high entropy alloys according to specific requirements.

The results of our hardness testing and compression tests unveiled significant disparities in mechanical properties between the two sets of samples. As the densification increased, the hardness and compression strength decreased, despite not being a significant difference. This underscores the pivotal role of densification in shaping the mechanical characteristics of high entropy alloys. The promising mechanical properties exhibited by the highly densified samples suggest their potential application in demanding engineering applications.

In the future, further tests may be conducted to complement the existing research. Namely, Scanning Electron Microscopy (SEM), Electron Backscatter Diffraction (EBSD), and Transmission Electron Microscopy (TEM). SEM provides high-resolution images of HEA microstructures. Combined with energy-dispersive X-ray spectroscopy (EDS), it can also reveal the distribution of elements and phases within the alloy. EBSD can be used to characterize the microstructure, crystallography, and grain boundaries within HEAs. It's especially useful for understanding grain orientation and texture. This technique is the most appropriate one to identify the boundaries in the material as well as its elements.TEM allows for even higher resolution imaging and can provide detailed information on the microstructure, including grain boundaries, defects, and phases at the nanoscale.

In summary, this study has contributed to the evolving field of additive manufacturing of high entropy alloys. By comparing optical microscopy, hardness testing, and compression tests with varying levels of densification, we have unveiled the significance of densification in tailoring microstructural and mechanical properties. The potential for high-performance applications is evident, and the pursuit of these avenues promises to open exciting prospects in material science and engineering.

This research underscores the importance of interdisciplinary collaboration between materials scientists, engineers, and additive manufacturing experts, forging a path towards innovative materials that can meet the evolving demands of modern industry.

BIBLIOGRAPHY

[1] Y. Zhang *et al.*, "Microstructures and properties of high-entropy alloys," *Progress in Materials Science*, vol. 61. Elsevier Ltd, pp. 1–93, 2014. doi: 10.1016/j.pmatsci.2013.10.001.

[2] J. Chen *et al.*, "A review on fundamental of high entropy alloys with promising high–temperature properties," *Journal of Alloys and Compounds*, vol. 760. Elsevier Ltd, pp. 15–30, Sep. 05, 2018. doi: 10.1016/j.jallcom.2018.05.067.

[3] B. Cantor, I. T. H. Chang, P. Knight, and A. J. B. Vincent, "Microstructural development in equiatomic multicomponent alloys," *Materials Science and Engineering A*, vol. 375–377, no. 1-2 SPEC. ISS., pp. 213–218, Jul. 2004, doi: 10.1016/j.msea.2003.10.257.

[4] J. W. Yeh *et al.*, "Nanostructured high-entropy alloys with multiple principal elements: Novel alloy design concepts and outcomes," *Adv Eng Mater*, vol. 6, no. 5, pp. 299–303, 2004, doi: 10.1002/adem.200300567.

[5] J. G. Lopes and J. P. Oliveira, "A short review on welding and joining of high entropy alloys," *Metals*, vol. 10, no. 2. MDPI AG, 2020. doi: 10.3390/met10020212.

[6] S. S. Nene, M. Frank, K. Liu, R. S. Mishra, B. A. McWilliams, and K. C. Cho, "Extremely high strength and work hardening ability in a metastable high entropy alloy," *Sci Rep*, vol. 8, no. 1, Dec. 2018, doi: 10.1038/s41598-018-28383-0.

[7] J. P. Oliveira *et al.*, "Gas tungsten arc welding of as-rolled CrMnFeCoNi high entropy alloy," *Mater Des*, vol. 189, Apr. 2020, doi: 10.1016/j.matdes.2020.108505.

[8] J. Li, X. Meng, L. Wan, and Y. Huang, "Welding of high entropy alloys: Progresses, challenges and perspectives," *Journal of Manufacturing Processes*, vol. 68. Elsevier Ltd, pp. 293–331, Aug. 01, 2021. doi: 10.1016/j.jmapro.2021.05.042.

[9] S. S. Nene *et al.*, "Reversed strength-ductility relationship in microstructurally flexible high entropy alloy," *Scr Mater*, vol. 154, pp. 163–167, Sep. 2018, doi: 10.1016/j.scriptamat.2018.05.043.

[10] S. Thapliyal *et al.*, "Segregation engineering of grain boundaries of a metastable Fe-Mn-Co-Cr-Si high entropy alloy with laser-powder bed fusion additive manufacturing," *Acta Mater*, vol. 219, Oct. 2021, doi: 10.1016/j.actamat.2021.117271.

[11] M. Orme, I. Madera, M. Gschweitl, and M. Ferrari, "Topology optimization for additive manufacturing as an enabler for light weight flight hardware," *Designs (Basel)*, vol. 2, no. 4, pp. 1–22, Dec. 2018, doi: 10.3390/designs2040051.

[12] M. Orme *et al.*, "A DEMONSTRATION OF ADDITIVE MANUFACTURING AS AN ENABLING TECHNOLOGY FOR RAPID SATELLITE DESIGN AND FABRICATION," 2016. [Online]. Available: https://www.researchgate.net/publication/306578773

[13] S. Kumar, A. Patnaik, A. K. Pradhan, and V. Kumar, "Effect of Cobalt Content on Thermal, Mechanical, and Microstructural Properties of Al0.4FeCrNiCox (x = 0, 0.25, 0.5, 1.0 mol) High-Entropy Alloys," *J Mater Eng Perform*, vol. 28, no. 7, pp. 4111–4119, Jul. 2019, doi: 10.1007/s11665-019-04162-4.

[14] K. V. Wong and A. Hernandez, "A Review of Additive Manufacturing," *ISRN Mechanical Engineering*, vol. 2012, pp. 1–10, Aug. 2012, doi: 10.5402/2012/208760.

[15] A. Lopez, R. Bacelar, I. Pires, T. G. Santos, J. P. Sousa, and L. Quintino, "Non-destructive testing application of radiography and ultrasound for wire and arc additive manufacturing," *Addit Manuf*, vol. 21, pp. 298–306, May 2018, doi: 10.1016/j.addma.2018.03.020.

[16] P. Kruth, "Material Incress Manufacturing by Rapid Prototyping Techniques."

[17] U. M. Dilberoglu, B. Gharehpapagh, U. Yaman, and M. Dolen, "The Role of Additive Manufacturing in the Era of Industry 4.0," *Procedia Manuf*, vol. 11, pp. 545–554, 2017, doi: 10.1016/j.promfg.2017.07.148.

[18] M. Munsch, "Laser additive manufacturing of customized prosthetics and implants for biomedical applications," in *Laser Additive Manufacturing: Materials, Design, Technologies, and Applications*, Elsevier Inc., 2017, pp. 399–420. doi: 10.1016/B978-0-08-100433-3.00015-4.

[19] L. E. Murr *et al.*, "Microstructure and mechanical behavior of Ti-6Al-4V produced by rapid-layer manufacturing, for biomedical applications," *Journal of the Mechanical Behavior of Biomedical Materials*, vol. 2, no. 1. pp. 20–32, Jan. 2009. doi: 10.1016/j.jmbbm.2008.05.004.

[20] M. E. Orme *et al.*, "Additive manufacturing of lightweight, optimized, metallic components suitable for space flight," in *Journal of Spacecraft and Rockets*, American Institute of Aeronautics and Astronautics Inc., 2017, pp. 1050–1059. doi: 10.2514/1.A33749.

[21] S. Mellor, L. Hao, and D. Zhang, "Additive manufacturing: A framework for implementation," in *International Journal of Production Economics*, Mar. 2014, pp. 194–201. doi: 10.1016/j.ijpe.2013.07.008.

[22] J. A. Scott, "Additive Manufacturing: Status and Opportunities," 2012. [Online]. Available: https://www.researchgate.net/publication/312153354

[23] P. Agrawal, S. Thapliyal, S. S. Nene, R. S. Mishra, B. A. McWilliams, and K. C. Cho, "Excellent strength-ductility synergy in metastable high entropy alloy by laser powder bed additive manufacturing," *Addit Manuf*, vol. 32, Mar. 2020, doi: 10.1016/j.addma.2020.101098.

[24] P. Agrawal *et al.*, "Metastable high entropy alloys: An excellent defect tolerant material for additive manufacturing," *Materials Science and Engineering: A*, vol. 826, Oct. 2021, doi: 10.1016/j.msea.2021.142005.

[25] V. Mahato, M. A. Obeidi, D. Brabazon, and P. Cunningham, "Detecting voids in 3D printing using melt pool time series data," *J Intell Manuf*, vol. 33, no. 3, pp. 845–852, Mar. 2022, doi: 10.1007/s10845-020-01694-8.

[26] X. Xiao, C. Lu, Y. Fu, X. Ye, and L. Song, "Progress on Experimental Study of Melt Pool Flow Dynamics in Laser Material Processing." [Online]. Available: www.intechopen.com

[27] K. C. Mills, B. J. Keene, R. F. Brooks, and A. Shirali, "Marangoni effects in welding," *Philosophical Transactions of the Royal Society A: Mathematical, Physical and Engineering Sciences*, vol. 356, no. 1739, pp. 911–925, Apr. 1998, doi: 10.1098/rsta.1998.0196.

[28] M. Bahramyan, R. T. Mousavian, and D. Brabazon, "Study of the plastic deformation mechanism of TRIP-TWIP high entropy alloys at the atomic level," *Int J Plast*, vol. 127, 2020, doi: 10.1016/j.ijplas.2019.102649.

[29] R. W. Evans and P. J. Scharning, "Axisymmetric compression test and hot working properties of alloys."

[30] B. Bellón, S. Haouala, and J. Llorca, "An analysis of the influence of the precipitate type on the mechanical behavior of Al-Cu alloys by means of micropillar compression tests."

[31] G. Laplanche *et al.*, "Elastic moduli and thermal expansion coefficients of medium-entropy subsystems of the CrMnFeCoNi high-entropy alloy," *J Alloys Compd*, vol. 746, pp. 244–255, May 2018, doi: 10.1016/j.jallcom.2018.02.251.

⟨year⟩ JOHN DOE A VERY LONG AND IMPRESSIVE THESIS TITILE WITH A FORCED LINE BREAK

NOVA SCHOOL OF SCIENCE & TECHNOLOGY